Fishery Technology 61 (2024) : 133 - 143

Mitigating Lead Pollution in Marine Ecosystems: Nano-Silica-Reinforced Epoxy Coating for Enhanced Corrosion Resistance of Fishing Sinkers

Shifa Jalal[1,2], K. R. Vrindha[1], P. Muhamed Ashraf[1*] and M. P. Remesan[1]
[1] *ICAR Central Institute of Fisheries Technology, Kochi, Kerala - 682 029*
[2] *School of Chemical Sciences, Mahatma Gandhi University, Kottayam, Kerala - 686 560*

Abstract

Lead sinkers are a popular choice among fishers due to their affordability, ease of manufacture, density, and chemical stability. However, their widespread use has contributed to environmental pollution, particularly in marine ecosystems, resulting from leaching, abrasion, and degradation. The present study aims to address lead contamination from fishing sinkers in the marine environment by utilizing nano silicon dioxide-reinforced bisphenol A epoxy polymeric coating on the lead and assessing the coating's resistance to corrosion. The reinforcement of SiO_2 was confirmed through UV-Vis spectroscopy and FTIR, demonstrating the SiO_2 interacting with the benzene moiety of the bisphenol A epoxy resin. The SiO_2 was uniformly distributed in the epoxy resin, resulting in a pore free and a smoother surface. Electrochemical evaluation showed that 0.5% SiO_2 reinforcement in epoxy resin was optimal for enhancing corrosion inhibition. The abrasion resistance of lead coated with nano SiO_2-epoxy resin exhibited efficiencies of 50.18% and 88.71%, respectively, with SiO_2-epoxy coating thicknesses of 0.011 mm and 0.033 mm, compared to the untreated control. The potential impact of these results on the marine environment could be significant, as they may provide a more environmentally friendly and economical option for fishers who rely on lead sinkers.

Keywords: Lead pollution, sinkers, epoxy resin, nano silicon dioxide, corrosion,

Received 29 January 2024; Revised 18 March 2024; Accepted 1 April 2024

Email: ashrafp2008@gmail.com

Introduction

A fishing sinker is a weight, typically made of lead, which is used in conjunction with fishing lures to increase their sinking speed, anchoring stability, and/or casting distance. Fishing sinkers come in a variety of weights, shapes, and sizes to suit different fishing applications. Lead is the preferred choice as sinker for commercial and recreational fishing operations due to its low cost, ease of moulding and fabrication, chemical inertness, and density. However, lead is a potential pollutant in the environment, and there are concerns about its use as a sinker in fishing gear. Lead can be introduced to aquatic environments by inevitable occasional loss and leaching of lead sinkers (Grade et al., 2019). Taking these issues in concern, countries like USA, Canada, and UK banned the use of lead sinkers in fishing (Thomas & Guitart, 2010). These bans have inspired to search for other alternatives like steel, brass, sand, tungsten, carbon and bismuth sinkers, but it was not widely adopted due to their density difference and increased cost compared to lead (Grade et al., 2019). In addition, leaching and degradation of lead sinkers have resulted in low efficiency and economic loss to the fishers. Although lead is still used for various fishing gear operations, it is important to find an alternative strategy to prevent the leaching of lead into the environment.

Nanostructured hydrophobic and super-hydrophobic coatings of primers are explored to reduce metallic corrosion (Zhang et al., 2016; Xiang et al., 2018). Epoxy resins are extensively employed as a coating material in metals since it acts as an efficient barrier against the penetration of corrosives and also exhibited excellent mechanical strength, chemical inertness, good insulation, strong adhesion to heterogeneous substrates, and cheaper in cost (Qiu et al., 2017). Epoxy coatings also act as a reservoir

for corrosion inhibitors, which help the metal surface fend off attacks from noxious species such as elevated chloride ion concentrations, O_2 or H^+ (Conradi et al., 2015). However the poor impact and stress cracking resistance of epoxy coatings, which result from their strongly cross-linked structure and aggressive ions penetrating through the resin pores (Corvo et al., 2008), as well as their vulnerability to surface degradation by surface abrasion and wear (Wetzel et al., 2003), severely restrict their usage in industry.

Recent years have seen a rise in research into the polymer nanocomposites fabricated by reinforcing inorganic or organic fillers into the organic polymers (Guan et al., 2018; Alam et al., 2018). The inherent qualities of composites are largely influenced by their size, shape, morphology, and filler weight percentage. Silica, alumina, and titania nanoparticles are well-known inorganics employed in coating formulations (Mora et al., 2017; Ledwig & Dubiel, 2017; Ershad-Langroudi et al., 2017). Due to their distinctive characteristics, nanoparticles have been employed to improve the mechanical, thermal, and corrosion resistance of metal matrices (Radhamani et al., 2020). The characteristics of polymeric resin can be enhanced by adding more phase-inorganic fillers. By adding inorganic nanoparticles to the resins, the microsites will be filled, which will enhance the forces that interact at the polymer-filler interfaces. Well-distributed nanoparticles will efficiently improve the comprehensive properties of nanocomposites, which are unique and different from any other composites. Nano silicon dioxide (SiO_2) is one of the frequently used additives in epoxy resins, since the composite exhibit improved adhesion, corrosion resistance, less toxic, and abrasion resistance, and hence preferred in paints, sealants, adhesives etc. (Wetzel et al., 2003; Zhang et al., 2002; Rong et al., 2003; Matejka et al., 2000). Zhou et al. (2003, 2004) and Kinloch & Taylor, (2003) compared nano and micro sized particles reinforced epoxies and the latter showed superior thermal and mechanical properties. It is common knowledge that the load placed on composite materials is primarily passed to the fillers through an interface. As reported by Elfakhri et al. (2022), increasing the amount of fillers and specific surface area enhances the mechanical and impact properties of composites.

Despite the widespread use of lead sinkers in recreational and commercial fishing, their protection from corrosion and abrasion in marine environments has received little attention. This study presents a novel approach to tackling this issue by synthesizing a nano SiO_2 reinforced bisphenol epoxy polymer and applying it as a coating for lead sinkers. The study not only investigates the interaction between lead and the epoxy polymer but also examines the corrosion and abrasion resistance of the coated lead sinkers. The outcome of the study is expected to reduce lead degradation and economic benefits to fishers.

Materials and Methods

Lead sheet (Pb 99.9%) of 2 mm thickness was purchased from MKR X-Ray Products, Kochi, India. Bisphenol A diglycidyl ether (Epoxy resin) and poly (propyleneglycol) bis (2-aminopropyl ether) as curing agent was procured from Sigma Aldrich, Singapore. Hydrophilic nano-silica powder was purchased from Reinste Nano Ventures Private Ltd., New Delhi, India. Sodium Chloride required for corrosion studies was supplied by Central Drug House (P) Ltd., New Delhi, India.

Corrosion rates of lead samples by weight loss method were evaluated in six samples of lead coupons of size 5 cm x 2.5 cm after surface cleaning using SiC paper up to 1000 grits, cleaned by using water and acetone through ultra-sonication. The samples were weighed out using 0.01 mg accuracy by using Sartorius 211D electronic balance. Three numbers of each sample were immersed in 3.5% NaCl and natural seawater of 29.06 psu for 40 days in the laboratory at a room temperature of 27±3°C (ASTM G1). After the time period it was taken out and weighed accurately. As per ASTM G1, the samples were acid washed by boiling the samples in a solution of 5 mL acetic acid in 500 mL distilled water for 5 min. to remove corrosion products, dried in oven, cooled by keeping in desiccator and weighed again. Corrosion rate was determined according to the equation

Corrosion rate mm yr^{-1}= KW/ (ATD) --------- (1)

Where K is the corrosion constant, W is the mass loss, T is the time of exposure in hours, A is the area in cm^2 and D is the density of the matrix.

Hydrophilic nano-silica powder was weighed out accurately and mixed with epoxy resin so as to obtain 0.05, 0.1, 0.2, 0.5 and 1% by weight nano-silica epoxy composite and was sonicated for homogeniz-

ing the mixture. Hardener was added to the resin mixture (1:2) and stirred well for 5 min. To remove air bubble, the mixture was sonicated for 5 min and an untreated control was prepared without adding nano SiO_2.

Lead coupons of 5 cm × 2.5 cm size were surface processed by polishing with SiC paper down to 1000 grit, and then rinsed with acetone and water to get a silvery surface profile. A known volume of composite was dropped over the lead specimens, coating uniformity was ensured by keeping a polyethylene sheet and a glass slide over the film. The lead with epoxy layer of coating was cured for 4 h at 50°C. The coating thickness, measured using micrometer, was found to be around 0.164 mm.

Lead samples with untreated control coating and 1% nano SiO_2 epoxy composite coating were characterized by using Shimadzu 2450 double beam UV-Visible spectrophotometer fitted with integrating sphere accessory. A non-coated lead sample was kept as reference and scanned at 800-200 nm wavelength. Fourier Transform Infrared (FTIR) spectra were recorded by using Thermo Nicolet iS10 FTIR fitted with Zn-Se iTR accessory. The samples were scanned from 650 to 4000 cm^{-1}. The coated samples (control and 1% nano-silica epoxy composite coating) were observed under the light microscope (Leica MZ16A Stereo Microscope) at 15, 25, 50 and 100X magnifications and further characterized by Scanning Electron Microscope (Jeol/JEM2100 and Model JSM-6390LV).

The electrochemical impedance spectroscopic measurements were carried out by using Autolab 302N electrochemical system fitted with FRA module and the generated data was processed using the NOVA software. The electrochemical cell used for this study consists of lead coated with different concentrations of nano SiO_2 epoxy composite as working electrode, platinum as auxillary electrode, Ag/AgCl (3M KCl) as reference electrode and 3.5% NaCl as electrolyte. The treatment details of the samples are as follows: R0, control; R1, 0.05%; R2, 0.1%; R3, 0.2%; R4, 0.5%; and R5, 1% SiO_2 reinforced epoxy polymer composite. The experiment was repeated 3 times for each concentration. Linear polarization studies were carried out by exposing 1 cm2 area of epoxy coated lead panels in 3.5% sodium chloride electrolyte as the working electrode, Pt as counter electrode, and Ag/AgCl (3 M KCl) as reference electrode. Voltage scanned from ±0.5 V with respect to open circuit potential (OCP), with a step potential of 0.005 V and a scan rate of 0.005 Vs^{-1}.

The abrasion testing machine simulates abrasion condition which is used to evaluate the effect of abrasion resistance. The test method for abrasion resistance was conducted as per ISO 4649 / DIN 53516. The weights of the lead samples with coating were recorded using a 0.01 mg sensitive Sartorius balance. The pre weighed nano SiO_2 epoxy coated and untreated control epoxy lead panels were placed over the rolling drum of abrasion tester for 1000 cycles at constant speed. The strings fixed with lead were hanged with equal weight to enable uniform placement over the rolling drum. After completion of 1000 cycles the samples were weighed again. Aggregate abrasion value = ((A-B)/B) × 100%, where A and B respectively represents initial and final weight of the lead samples.

Result and Discussion

A preliminary evaluation was conducted on lead coupons to gain a better understanding of the corrosion characteristics of the lead sheets. Lead coupons exposed to natural seawater and 3.5% NaCl solutions exhibited corrosion rates of $6.20\times10^{-3} \pm 2.13\times10^{-3}$ and $9.12\times10^{-3} \pm 8.39\times10^{-3}$ mmpy respectively. These findings suggest that the passivation mechanisms at work in these two solutions may be different, as seawater contains various anions (Cl^-, SO_4^{2-}, HCO_3^-, CO_3^{2-}, etc.) while NaCl only contains Cl^-. Understanding the differences in corrosion rates and mechanisms in these solutions is important for developing effective strategies to minimize lead corrosion in marine environments. Linear sweep voltammetric study revealed the corrosion potential (E_{corr}), Corrosion current density (I_{corr}) and polarisation resistance (R_p) respectively was -0.696 ± 0.003 V, $4.90\times10^{-5} \pm 2.77\times10^{-5}$ Acm^{-2}, 484 ± 66 Ω cm^2. The low R_p and high I_{corr} clearly indicated the poor corrosion resistance of lead in the marine environment. Electrochemical impedance (EIS) studies exhibited constant phase element (CPE) $1.71\times10^{-5} \pm 6.90\times10^{-6}$ F, and polarization resistance (R_p) 190 ± 121 Ω cm^2 in the high frequency (HF) domain and the CPE and R_p in low frequency (LF) domain respectively was 2610 ± 696 Ω cm^2. The EIS data of LF domain highlighted the behaviour of internal layer of the lead and HF domain showed the behaviour of the outermost layer, lead oxide. The high capacitance and low R_p values indicated the lead was highly susceptible to corrosion in the

marine environment. This further correlated with the results of weight loss studies, highlighting the need to protect lead sinkers from direct exposure to the marine environment.

The synthesis of a nano SiO_2-Bisphenol A composite was standardized, and different amounts of nano SiO_2 were used to reinforce Bisphenol A epoxies. The resulting reinforced epoxies were coated over lead panels and the optimum curing temperature was found to be between 40-50°C for a duration of 4 hours. The cured coating in hot air oven was characterized using UV-Visible and FTIR spectroscopy, and it was also found to be corrosion-resistant through electrochemical testing.

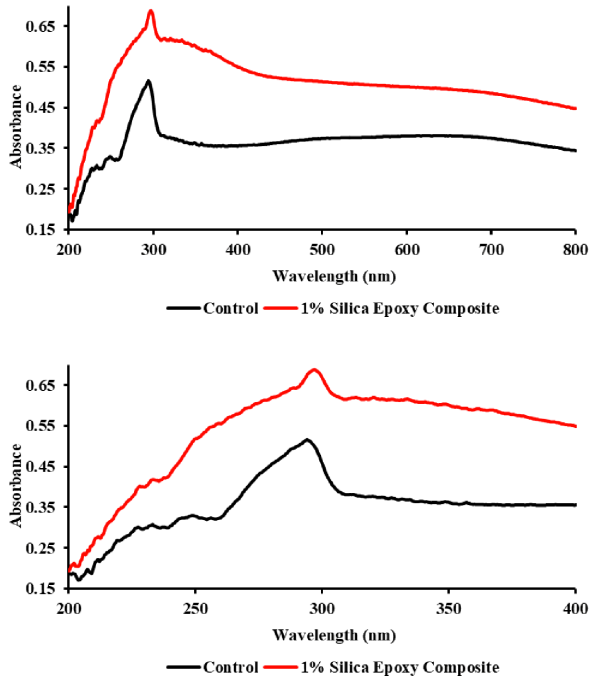

Fig. 1. UV-Visible spectra of epoxy resin (black) and 1% nano silica epoxy composite (red).

UV-Visible spectroscopic analysis (Fig. 1) provides information on changes in the characteristic absorption of molecules resulting from changes in molecular characteristics and different treatments. The control sample displayed a l_{max} at 226, 288, and 242 nm, while the SiO_2 reinforced epoxy polymer was 231, 293, and 336 nm. Compared to the control, SiO_2 reinforced epoxy polymer exhibited many minor absorptions and some of the absorptions of untreated were missing in the composite. The data revealed that the addition of nano-SiO_2 to the epoxy resin caused a red shift in its absorption. These deviations in the spectra can be attributed to the interaction of SiO_2 with the epoxy polymer in the $\pi - \pi^*$ system, indicating the successful formation of the composite.

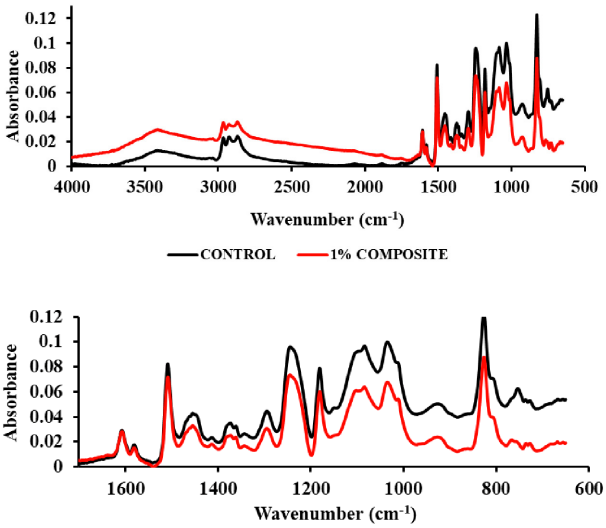

Fig. 2. a) FTIR spectra of epoxy resin (black) and 1% composite (red); b) expanded version of the spectra of range 1700-650 cm^{-1}

The FTIR evaluation of epoxy resin and nano-SiO_2 reinforced epoxy resin was carried out, and the details are shown in Table 1 and Fig. 2. The profile indicated most of the peaks pertaining to the epoxy resin. The FTIR spectra exhibited peaks of the oxirane group at 825, 859, 918 cm^{-1} and a very small peak at 3060 cm^{-1} could be attributed to C-H stretch of the terminal oxirane group. The broad band at 3500 cm^{-1} was assigned to O-H stretching of hydroxyl groups, revealing the presence of dimers or high molecular weight species. There was also a strong band corresponding to the ether linkage located at 1240 cm^{-1}. The epoxy resin exhibited a triplet of aromatic C-H out-of-plane stretching absorption from 726 to 760 cm^{-1}, while the nano SiO_2 reinforced epoxy resin exhibited five peaks within the same region indicating C-H stretching in varied environments (Table 1) due to the influence of nano SiO_2. The hydrogen bond of OH stretch is however showing a significant shift in the nanocomposite resin. This was due to the interaction of nano SiO2 with the OH groups of epoxy resin. The result showed the SiO_2 was interacting with the aromatic ring of bisphenol A. The characteristics absorption of Si-O-Si expected around 1090 and 1050 cm^{-1}, and

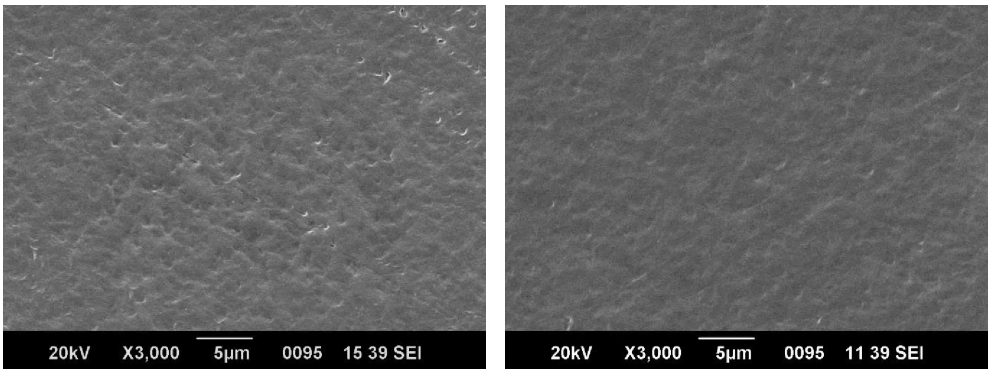

Fig. 3. Scanning electron micrographs of a) Bisphenol A, and b) nano SiO_2 reinforced Bisphenol A epoxy composite coated lead samples.

the aromatic C-H also exhibit multiplets around 1000 to 1150 cm^{-1}. In the present study, the aromatic C-H of bisphenol A absorption masked the SiO_2 absorption, and hence no distinct peak of the latter was shown except a shift in absorption from 1091 to 1095 cm^{-1}. The shift might be due to the interaction of SiO_2 with aromatic ring of bisphenol A. When SiO_2 surface was modified by using hexadecyltrimethoxysilane, the latter absorptions were masked by nano SiO_2 and showed a wider band (Xu & Zhang, 2021). In the present study, organic functional groups dominated when compared to SiO_2, and hence the latter absorptions were masked. It is confirmed that the nano silica particles are firmly interacting with the epoxy resin through the aromatic ring. This can be further correlated with the observations in UV-Vis spectroscopy.

The scanning electron micrographs of lead coated with epoxy and nano SiO_2 reinforced epoxy resin are shown in Fig. 3 a) and b) respectively. The addition of nano SiO_2 resulted in a surface that was found to be more pore-free, smoothed, and uniform. The addition of SiO_2 in the bisphenol A resin significantly decreased pores. Zhang et al. (2006) and Pham et al. (2017) studied the aliphatic epoxy resin reinforced with nano silica and showed improved toughness, thermal stability and crack resistance.

Electrochemical characteristics of epoxy and varied concentrations of nano SiO_2 reinforced epoxy coated lead samples have been studied by linear Sweep Voltammetry (LSV) and electrochemical Impedance Spectroscopy (EIS).

Tafel plots and the LSV characteristics of epoxy and SiO_2-epoxy coated lead panels were shown in Fig 4. The corrosion potential (E_{corr}), corrosion current density (I_{corr}) and polarisation resistance (R_p) varied from -0.722 ± 0.002 to -0.232 ± 0.168 V, $1.73\times10^{-10} \pm 1.32\times10^{-10}$ to $2.19\times10^{-7} \pm 3.12\times10^{-7}$ A cm^{-2} and $1.38\times10^{6} \pm 7.29\times10^{5}$ to $6.50\times10^{8} \pm 2.48\times10^{8}$ Ω cm^2 respectively. The highest E_{corr} was exhibited by the coupons coated with 0.5% nano SiO_2 – epoxy polymer composite. The lowest I_{corr} and the highest R_p were exhibited by the lead coupon coated with 0.5% SiO_2 reinforced epoxy composite (R4) indicating its highest corrosion resistance compared to other treatments. A further increase in the concentration of nano SiO_2 in the epoxy caused a detrimental effect on corrosion resistance. The Tafel plot clearly depicted similar results. Thus 0.5% nano silica reinforced epoxy composite was optimum for getting the highest corrosion resistance in marine environment. Incorporation of nano SiO_2 in the epoxy polymer exhibited improved corrosion resistance of steel and it was explained due to the improved physical barrier, and compactness of the uniformly distributed nano silica in the composite (Huang et al., 2011; Li et al., 2012). The improved corrosion resistance in the lead was probably due to the increased physical barrier of epoxy resin due to the reinforcement of nano SiO_2.

The EIS provides information to describe the electrochemical behaviour of the corrosion system. Electrode impedance is a complex number and the impedance spectra were normally displayed in a Nyquist plot, where the imaginary part of impedance (-Z″) is plotted against real part (Z″). The polarization resistance (R_p) value is inversely proportional to the corrosion rate of the system. This parameter provides an estimation of the protective efficiency of the composite. The experimental data

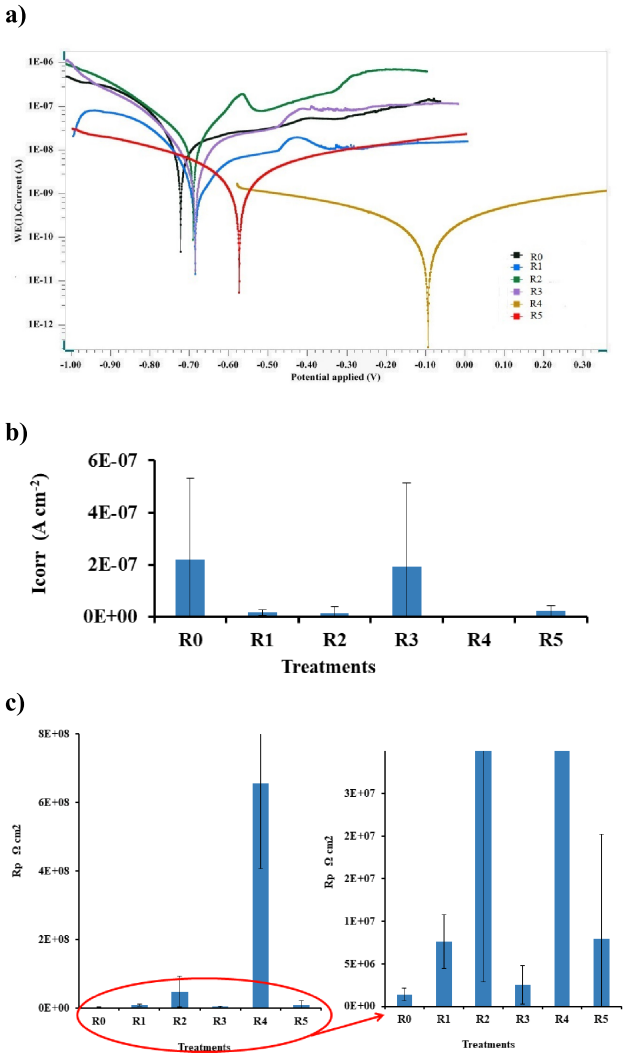

R0, Epoxy coated; R1, 0.05% SiO_2– epoxy coated; R2, 0.1% SiO_2– epoxy coated; R3, 0.2% SiO_2– epoxy coated; R4, 0.5% SiO2 – epoxy coated; R5, 1% SiO_2– epoxy coated.

Fig. 4. Electrochemical characteristics of epoxy and SiO2 reinforced epoxy coated lead. a) Tafel plot, b) Corrosion potential, and c) polarization resistance with respect to treatments with expanded view lower values.

can be described using an equivalent circuit. In this equivalent circuit, R_s is the solution resistance and R_p is the polarization resistance. A constant phase element (CPE) is introduced for better data fitting instead of an ideal capacitance parameter. The expression of CPE is defined by

$$Z_{CPE} = I/A\ (j\omega)^n \text{ ---------- } (2)$$

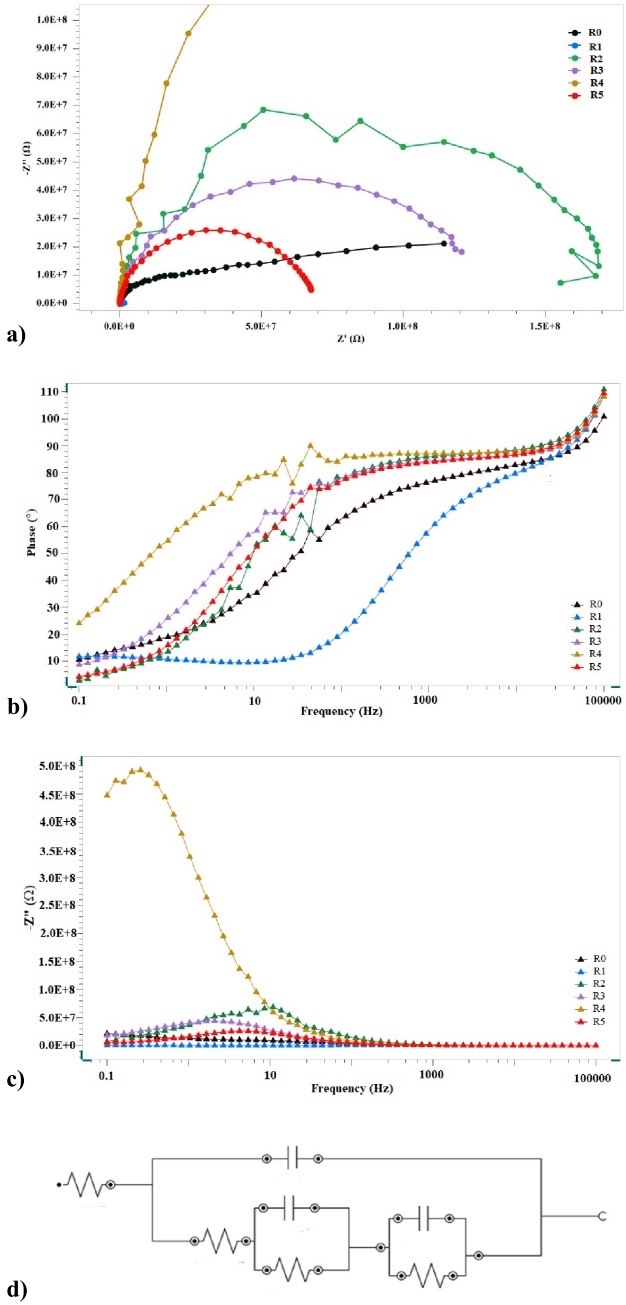

Fig. 5. a) Nyquist plot of treatments: R0, untreated; R1, 0.05%; R2, 0.1%; R3, 0.2%; R4, 0.5% and R5, 1%, b and c) Bode plots of treatments and d) Equivalent circuit used for fitting the EIS data.

Where A and n are the frequency- independent parameters, $j = (-1)^{1/2}$ and $\omega = 2\pi f$ the angular frequency.

The EIS data for the epoxy and SiO_2 reinforced epoxy polymer coated lead samples were shown in

Table 1. FTIR data of epoxy resin and Nano silica Epoxy Composite

Bisphenol A Epoxy polymer (Wavenumber cm^{-1})	Nanosilica- Epoxy Composite (Wavenumber cm^{-1})	Functional Groups
726	724, 728	Ar C-H out of plane
750	752, 758	"
760	762	"
804	802	1,4 disubstituted para
825	825	Stretching C-O-C of oxirane group
859	859	Epoxy ring
918	919	Stretching C-O of oxirane group
1010	1009	Aromatic C-H stretch
1030	1030	Si-O-Si
1080	1080	Aromatic C-H stretch
1091	1095	Si-O-Si
1141	1141	Aromatic C-H stretch
1179	1179	Aromatic O-H
1238	1240	Aryl O stretch ether
1291	1290	Aromatic Secondary Amine
1334	1334	CN stretch
1359	1359	CH stretch
1370	1368	Geminal dimethyl group
1408	1406	O-H bend/ stretch
1448	1450	Aromatic ring
1507	1507	Aromatic C-C stretch
1578	1578	Secondary NH
1610	1606	Stretching C=C of Benzene ring
2958-2856	2956-2856	C-H str of CH_2 and CH_3
3060	3060	C-H stretching of terminal oxirane group
3685-3193	3695-3203	H- bonded OH stretch

Fig 5 and Table 2. The data was fitted with an equivalent circuit model **(Rs(C1[R1(C2R2)](C3R3))** as shown in Fig. 5. In the circuit, R_s is the solution resistance, R1=R_p1 is the polarisation resistance and C1= C1 is the constant phase element in high frequency region and R2+R3= R_p2 is the polarisation resistance and C2+C3= CPE2 is the constant phase element in low frequency region. The low frequency domain polarisation resistance (R_2 and R_3) and capacitance (C2 and C3) values were added for making convenience in the discussion. The Nyquist plot and Bode plots are shown in Fig. 5b. In high frequency region, the C1 and R_p1 ranged from 1.98×10^{-10} $\pm7.59\times10^{-11}$ to 2.31×10^{-8} $\pm3.96\times10^{-8}$ F and 8.43×10^{5} $\pm1.05\times10^{6}$ to 1.41×10^{8} $\pm1.23\times10^{8}$ Ω cm^2 respectively. Similarly C_2 and R_p2 in low frequency region varied from 4.14×10^{-10} $\pm2.6\times10^{-10}$ to 9×10^{-8} $\pm1.52\times10^{-7}$ F and 1.90×10^{7} $\pm1.71\times10^{7}$ to 5.3×10^{8} $\pm4.08\times10^{8}$ Ω cm^2 respectively. The lowest CPE and highest R_p in high and low frequency region were showed for 0.5% nano silica reinforced epoxy composite (R4). This showed that the surface and internal layers of the lead was having improved corrosion resistance due to the composite coating. The Nyquist plot and the Bode plots (Fig. 5) depicted high corrosion resistance for R4. The Bode

Table 2. EIS data of different SiO_2 reinforced epoxy resin treatments after fitted with equivalent circuit model

Treatments	High frequency Domain		Low Frequency Domain	
	Constant Phase Element, C1 (F)	Polarisation Resistance, R_p1 (Ω cm^2)	Constant Phase Element, C2 (F)	Polarisation Resistance, R_p2 (Ω cm^2)
R0	$1.98x10^{-10} \pm 7.6x10^{-11}$	$8.43x10^{5} \pm 1.05x10^{6}$	$6.35x10^{-9} \pm 6.56x10^{-9}$	$3.2x10^{7} \pm 2.6x10^{7}$
R1	$2.31x10^{-8} \pm 3.96x10^{-8}$	$1.15x10^{7} \pm 1.94x10^{7}$	$9x10^{-8} \pm 1.52x10^{-7}$	$2.85x10^{8} \pm 4.91x10^{8}$
R2	$8.56x10^{-9} \pm 1.47x10^{-8}$	$3.13x10^{6} \pm 2.80x10^{6}$	$1.36x10^{-9} \pm 1.37x10^{-9}$	$1.22x10^{8} \pm 1.04x10^{8}$
R3	$2.13x10^{-10} \pm 9.6x10^{-11}$	$5.33x10^{6} \pm 1.67x10^{6}$	$1.36x10^{-9} \pm 9.88x10^{-10}$	$8.44x10^{7} \pm 5.65x10^{7}$
R4	$9.47x10^{-10} \pm 1.36x10^{-9}$	$1.41x10^{8} \pm 1.23x10^{8}$	$4.14x10^{-10} \pm 2.6x10^{-10}$	$5.3x10^{8} \pm 4.08x10^{8}$
R5	$1.05x10^{-9} \pm 1.21x10^{-9}$	$1.53x10^{7} \pm 1.52x10^{7}$	$3.23x10^{-8} \pm 5.28x10^{-8}$	$1.90x10^{7} \pm 1.71x10^{7}$

R0, Epoxy coated; R1, 0.05% SiO2 – epoxy coated; R2, 0.1% SiO_2 – epoxy coated; R3, 0.2% SiO2 – epoxy coated; R4, 0.5% SiO2 – epoxy coated; R5, 1% SiO2 – epoxy coated.

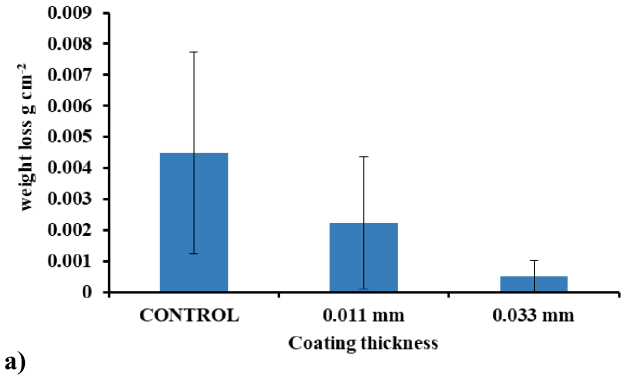

a)

b)

c)

Fig. 6. Abrasion test data of 0.5% SiO_2 reinforced bisphenol A epoxy polymer coated lead in two different thickness after 1000 cycles of operation in abrasion tester. b) composite coated arranged in the abrasion tester drum. c) nano SiO_2 – epoxy polymer coated lead sinkers.

plot of R4 was distinctly different from other treatments. Similar situations were experienced in Bode plots when a product formed after a reaction, indicating the formed composite was in high efficiency and optimum. This implied that the SiO_2 reinforced epoxy coated lead surface experienced lowest charge transfer spots and anodic dissolution of metal oxide due to the coating. On examining the Nyquist plot, there exhibited a disturbance in the middle frequencies which was reflected in previous studies by Ashraf et al. (2023) on nano carbon dot reinforced bisphenol epoxy polymer composite. The

reason is not known. The 0.5% nano SiO_2 – epoxy composite exhibited increased corrosion resistance evidenced by improved surface and internal layers due to the coating of composite over the lead.

The epoxy polymers may develop pores and cracks during the curing process, potentially reducing corrosion resistance when applied to a metallic substrate (Liu et al., 2023). Reinforcement of SiO_2 or similar additives in epoxy polymers will seal the pores and hinder the penetration of corrosives onto the coated surface (Verma et al., 2020). In the bisphenol A epoxy polymer the reinforced SiO_2 interacted with the aromatic ring of bisphenol A glycidyl moiety (Skachkova et al., 2013). The present study also revealed the SiO_2 was interacted with the aromatic rings of bisphenol A system. The treatment R4 demonstrated significantly higher corrosion resistance, likely because the optimal SiO_2 concentration uniformly distributed across the polymeric surface, as evidenced by SEM characterization. Moreover, an increased SiO_2 in the matrix resulted lower Rp, possibly due to the aggregation of excess SiO_2 within the matrix. The SiO_2 reinforcement in the epoxy polymer improved the electrochemical properties and corrosion resistance, this was attributed to the synergistic influence of SiO_2 and epoxy polymer.

The epoxy coated and nano SiO_2- epoxy coated lead panels in two thicknessess 0.011 and 0.033 mm were subjected to abrasion for 1000 cycles and the results are shown in Fig. 6. The results showed that the abrasion resistance of nano SiO2-epoxy resin exhibited an efficiency of 50.18% and 88.71% respectively when compared with lead coated solely with epoxy, with SiO2-epoxy coating thicknesses of 0.011±0.003 mm and 0.033±0.009 mm. This implied that nano SiO_2- epoxy coating can minimize the abrasion of lead while dragging the net and thereby corrosion of lead. Further, it needs to understand the sinking characteristics of lead sinkers coated with epoxy resins. Reinforcement of nano silica, clay or nickel oxide in epoxy polymers has improved the abrasion resistance of the composite along with other properties (Madhup et al., 2017, 2015; Wang & Qiu, 2022). Alam et al. (2020) reported 5% nano SiO_2 reinforcement in epoxy coating improved heat stability, abrasion resistance, hardness and elastic modulus. The present findings also corroborated with improved abrasion resistance of nano SiO_2 – epoxy coating over lead panels.

The SiO_2 - epoxy coated sinkers were shown in Fig. 6c. The sinkers were given 3 layered coating by immersion method. The composites were coated uniformly with shining. To ensure a uniform coating, it is necessary to standardize the coating method, and subsequently, the results after fixing with trawl fishing nets should be evaluated.

Conclusion

Contamination of aquatic environments with lead is a major concern, as the metal is extensively used as sinkers for commercial and recreational fishing operations and is subject to degradation due to corrosion, abrasion, and loss. A nano SiO_2 reinforced Bisphenol A composite was synthesized, and its successful formation was confirmed by FTIR and UV-Visible spectral studies. The SiO_2 – epoxy coated lead panels exhibited pore free surface compared to the untreated control. Electrochemical studies with LSV and EIS clearly demonstrated the high corrosion resistance of the coating, with the optimum concentration found to be 0.5% nano SiO_2 reinforced epoxy resin composite. The SiO_2 –epoxy coated surface also exhibited excellent abrasion resistance. Field evaluation will provide more information on the potential for further improvements and the possibility of incorporating more abrasives.

Acknowledgements

The authors sincerely thank the Director, ICAR- Central Institute of Fisheries Technology and Head of Fishing Technology, and Microbiology, Fermentation and Biotechnology Division for providing facilities.

References

Alam, A., Zhang, Y., Kuan, HC., Lee, SH. and Ma, J. (2018) Polymer composite hydrogels containing carbon nanomaterials – morphology and mechanical and functional performance. Prog. Polym. Sci. 77: 1-18

Alam, M. A., Abdus Samad, U., Alam, M., Anis, A. and Al-Zahrani, S. M. (2020) Enhancement in nanomechanical, thermal, and abrasion properties of SiO2 nanoparticle-modified epoxy coatings. Coatings 10(4): 310

Ashraf, P. M., Anju, V. S., Binsi, P. K. and Joseph, T. C. (2023) A green extraction process of nanocarbon dots from prawn shells, and its reinforcement in epoxy polymers. J. Appl. Polym. Sci. e53250

Conradi, M., Kocijan, A., Zorko, M. and Verpoest, I. (2015) Damage resistance and anticorrosion properties of nanosilica-filled epoxy-resin composite coatings. Prog. Org. Coat. 80: 1-7

Corvo, F., Pérez, T., Dzib, L. R., Martín, Y., Castañeda, A., González, E. and Pérez, J. (2008) Outdoor–indoor corrosion of metals in tropical coastal atmospheres. Corros. Sci. 50: 220-230

Elfakhri, F., Alkahtani, R., Li, C. and Khaliq, J. (2022) Influence of filler characteristics on the performance of dental composites: A comprehensive review. Ceram. Int. 48(19): 27280-27294

Ershad-Langroudi, A., Abdollahi, H. and Rahimi, A. (2017) Mechanical properties of sol–gel prepared nanocomposite coatings in the presence of titania and alumina derived nanoparticles. Plastics, Rubber and Composites 46: 25-34

Grade, T., Campbell, P., Cooley, T., Kneeland, M., Leslie, E., MacDonald, B., Melotti, J., Okoniewski, J., Parmley, EJ., Perry, C., Vogel, H. and Pokras, M. (2019) Lead poisoning from ingestion of fishing gear: A review. Ambio. 48(9): 1023-1038

Guan, L. Z., Zhao, L., Wan, Y. J. and Tang, L. C. (2018) Three-dimensional graphene-based polymer nanocomposites: preparation, properties and applications. Nanoscale, 10: 14788-14811

Huang, T. C., Su, Y. A., Yeh, T. C., Huang, H. Y., Wu, C. P., Huang, K. Y., Chou, Y. C., Yeh, J-M. and Wei, Y. (2011) Advanced Anticorrosive Coatings Prepared from Electroactive Epoxy-SiO2 Hybrid Nanocomposite Materials. Electrochim. Acta. 56(17): 6142-6149

Kinloch, A. J. and Taylor, A. C. (2003) Mechanical and fracture properties of epoxy/inorganic micro- and nano-composites. J. Mater. Sci. 22: 1439-1441

Ledwig, P. and Dubiel, B. (2017) Microstructure and corrosion resistance of composite nc-TiO2/Ni coating on 316L steel. Arch Metall. Mater. 62: 2455-2460

Li, W., Tian, H. and Hou, B. (2012) Corrosion performance of epoxy coatings modified by nanoparticulate SiO2. Mater. Corros. 63(1): 44-53

Liu, L., Zhao, M., Pei, X., Liu, S., Luo, S., Yan, M., Shao, R., Sun, Y., Xu, W. and Xu, Z. (2023) Improving corrosion resistance of epoxy coating by optimizing the stress distribution and dispersion of SiO2 filler. Prog. Org. Coat. 179: 107522

Madhup, M. K., Shah, N. K. and Parekh, N. R. (2017) Investigation and improvement of abrasion resistance, water vapor barrier and anticorrosion properties of mixed clay epoxy nanocomposite coating. Prog. Org. Coat. 102: 186-193

Madhup, M. K., Shah, N. K. and Wadhwani, P. M. (2015) Investigation of surface morphology, anti-corrosive and abrasion resistance properties of nickel oxide epoxy nanocomposite (NiO-ENC) coating on mild steel substrate. Prog. Org. Coat. 80: 1-10

Matejka, L., Dukh, O. and Kolarik J (2000) Reinforcement of crosslinked rubbery epoxies by in-situ formed silica. Polymer 41(4): 1449-1459

Mora, L. V., Naik, S., Paul, S., Dawson, R., Neville, A. and Barker, R. (2017) Influence of silica nanoparticles on corrosion resistance of sol-gel based coatings on mild steel. Surf. Coat. Technol. 324: 368-375

Pham, T. D., Vu, C. M. and Choi, H. J. (2017) Enhanced Fracture Toughness and Mechanical Properties of Epoxy Resin with Rice Husk-based Nano-Silica. Polym. Sci. Series A. 59: 437-444

Qiu, S., Chen, C., Zheng, W., Li, W., Zhao, H. and Wang, L. (2017) Long-term corrosion protection of mild steel by epoxy coating containing self-doped polyaniline nanofiber. Synth. Met. 229: 39-46

Radhamani, A. V., Lau, H. C. and Ramakrishna, S. (2020) Nanocomposite coatings on steel for enhancing the corrosion resistance: A review. J. Compos. Mater. 54(5): 681-701

Rong, M. Z., Zhang, M. Q., Shi, G., Ji, Q. L., Wetzel, B. and Friedrich, K. (2003) Graft polymerization onto inorganic nanoparticles and its effect on tribological performance improvement of polymer composites. Tribol. Int. 36: 697-707

Skachkova, V. K., Lyubimov, A. V., Lyubimova, G. V., Gusev, M. N., Grachev, A. V., Lalayan, V. M., Shaulov, A. Yu. and Berlin, A. A. (2013) Optically transparent heat-resistant nanocomposites based on epoxy resin and silicon dioxide. Nanotechnologies Russ. 8(1-2): 92-98

Thomas, V. G. and Guitart, R. (2010) Limitations of European Union policy and law for regulating use of lead shot and sinkers: comparisons with North American regulation. Environ. Policy Gov. 20(1): 57-72

Verma, C., Olasunkanmi, L. O., Akpan, E. D., Quraishi, M. A., Dagdag, O., El Gouri, M., Sherif, E. M. and Ebenso, E. E. (2020) Epoxy resins as anticorrosive polymeric materials: A review. React. Funct. Polym. 156: 104741

Wang, S. and Qiu, Y. (2022) Synthesis of SiO2 nanoparticle epoxy resin composite and silicone-containing epoxy resin for coatings. Appl. Bionics Biomech. 2022: 8227529

Wetzel, B., Haupert, F. and Zhang, M. Q. (2003) Epoxy nanocomposites with high mechanical and tribological performance, Compos. Sci. Technol. 63(14): 2055–2067

Xiang, T., Han, Y., Guo, Z., Wang, R., Zheng, S., Li, S., Li, C. and Dai, X. (2018) Fabrication of inherent anticorrosion superhydrophobic surfaces on metals. ACS Sustain. Chem. Eng. 6: 5598-5606

Xu, B. and Zhang, Q. (2021) Preparation and properties of hydrophobically modified nano-sio2 with hexadecyltrimethoxysilane. ACS Omega 6(14): 9764-9770

Zhang, D., Wang, L., Qian, H. and Li, X. (2016) Superhydrophobic surfaces for corrosion protection: a review of recent progresses and future directions. J. Coat. Technol. Res. 13: 11-29

Zhang, M. Q., Ronga, M. Z., Yu, S. L., Wetzel, B. and Friedrich, K. (2002) Effect of particle surface treatment on the tribological performance of epoxy based nanocomposites. Wear 253(9–10): 1086-1093

Zhang, X., Xu, W., Xia, X., Zhang, Z. and Yu, R. (2006) Toughening of cycloaliphatic epoxy resin by nanosize silicon dioxide. Mater. Lett. 60(28): 3319-3323

Zhou, S., Wu, L., Shen, W. and Gu, G. (2004) Study on the morphology and tribological properties of acrylic based polyurethane/fumed silica composite coatings. J. Mater. Sci. 39: 1593-1600

Zhou, S. X., Wu, L. M., Sun, J. and Shen, W. D. (2003) Effect of nanosilica on the properties of polyester based polyurethane. J. Appl. Polym. Sci. 88(1): 189-193